H_2 Guaranteed Cost Control Design and Implementation for Dual-Stage Hard Disk Drive Track-Following Servos

Jianbin Nie, Richard Conway, and Roberto Horowitz

Computer Mechanics Laboratory
Mechanical Engineering
University of California, Berkeley, CA, USA

January 2, 2012

Abstract

This paper discusses the design and implementation of H_2 guaranteed cost control for dual-stage hard disk drive track-following servo systems. The proposed approach is based on H_2 guaranteed cost analysis, in which an upper bound on the worst-case H_2 performance of a discrete-time system with gain-bounded unstructured uncertainty is determined via several Riccati equations. Subsequently, the output feedback H_2 guaranteed cost control synthesis algorithm is presented by exploiting Riccati equation structure to reduce the number and complexity of the semi-definite programs (SDPs) that need to be solved. The presented control synthesis methodology is then applied to a hard disk drive with a PZT-actuated suspension. Experimental results on the actual disk drive validate our control design.

1 INTRODUCTION

Since the first magnetic drive was invented in the 1950s by IBM, the areal density of hard disk drives (HDDs) has been doubling roughly every 18 months [1], in accordance with Moore's law. As the storage density is pushed higher, the concentric tracks on the disk must be pushed closer together, which requires much more accurate positioning control of magnetic read/write heads. The current goal of the magnetic recording industry is to achieve an areal density of 4 terabits/in^2, which implies that the track width is required to be 25 nm. As a result, the 3σ value of the closed-loop position error signal (PES) during track-following control must be less than 2.5 nm.

In order to achieve the continuous increase of the data storage density, dual-stage actuation (DSA)—which combines the traditional voice coil motor (VCM) and an additional micro-actuator (MA)—has been proposed as a means of enhancing servo tracking performance by increasing the servo bandwidth [7]. The configurations of dual-stage actuators can be categorized into three groups according to the location of the secondary actuator: actuated suspension, actuated slider and actuated head. In this paper, we will focus on the control design of DSA servo systems with actuated suspensions.

As mentioned earlier, the relevant performance metric in a HDD is the standard deviation of the PES. Since the squared H_2 norm of a system can be interpreted as the sum of variances of the system outputs under the assumption that the system is driven by independent white zero mean Gaussian signals with unit covariance, the H_2 norm is a useful performance metric for HDDs. In addition, since there tend to be large variations in HDD dynamics due to variations in manufacture and assembly, it is not enough to achieve the desired level of performance for a single plant; the controller must guarantee the desired level of performance for a large set of HDDs. Thus, we are interested in finding a controller which can produce as small H_2 norm of closed-loop systems as possible over a set of HDDs [3, 9]. To characterize the worst-case performance of a set of HDDs, we use its H_2 guaranteed cost—an upper bound on the worst-case H_2 performance of a system with unstructured uncertainty. Using this characterization, we focus on the H_2 guaranteed cost control synthesis. In [2], the authors developed two control synthesis algorithms respectively through the solution of discrete Riccati equations (REs) and entirely based on the solution of a sequence of semi-definite programs (SDPs). Since the control synthesis algorithm using discrete REs are often significantly more computationally efficient and numerically robust than the one entirely using SDPs, we utilize the algorithm via the solution of REs presented in [2] to synthesize H_2 guaranteed cost control. For such a control synthesis algorithm, the output feedback H_2 guaranteed cost control problem is reduced to a full control problem by exploiting Riccati equation structure to reduce the number and complexity of SDPs that need to be solved.

In order to evaluate the effectiveness of the presented control technique, we apply it to a hard disk drive

with a PZT-actuated suspension. Moreover, the designed controller was implemented on this actual hard disk drive with a laser Doppler vibrometer (LDV) to measure the feedback signal [8].

The paper is organized as follows. Section 2 describes our dual-stage HDD servo system. In Section 3, the H_2 guaranteed cost analysis is provided. The control synthesis algorithm is presented in Section 4. The control implementation is discussed in Section 5. The conclusion is given in Section 6.

2 MODELING OF DUAL-STAGE HDD SERVOS

Figure 1 shows the picture of a PZT-actuated suspension provided by Hutchinson Technology, Inc. (HTI). Two yellow PZT actuators are placed near the root of the suspension. They generate a push-pull action when driven by differential voltages. Meanwhile, a leverage mechanism is utilized to convert and amplify this small actuation displacement into large head motion.

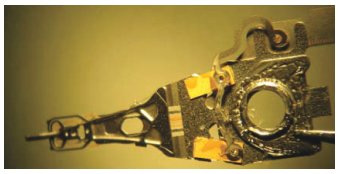

Figure 1: A PICTURE OF A PZT-ACTUATED SUSPENSION (PROVIDED BY HUTCHINSON TECHNOLOGY, INC..)

2.1 System Identification

In this paper, the DSA servo system is modeled as the block diagram shown in Fig. 2 in the same way as [8]. In Fig. 2, the windage is modeled as a white noise with scaled w_a; track runout r due to disk vibrations is modeled as a color noise; the measurement noise is assumed to be a white noise with scaled w_n. Notice that w_a, w_r and w_n have unit variance. The details of the modeling of σ_a, G_r and σ_n for the dual-stage servo system are demonstrated in [8]. The two actuators are represented by a nominal dual-input-single-output (DISO) system G_p with the output multiplicative uncertainty. W_Δ is the uncertainty weighting function and the unstructured uncertainty Δ is bounded with $\|\Delta\|_\infty \leq 1$.

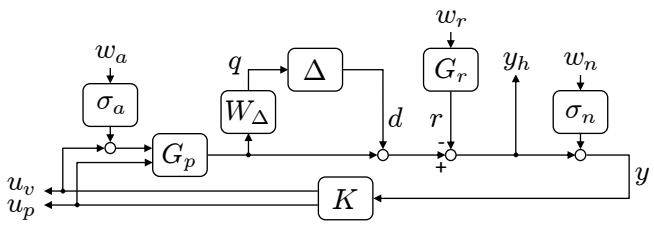

Figure 2: MODELING OF DUAL-STAGE HDD SERVO CONTROL SYSTEM

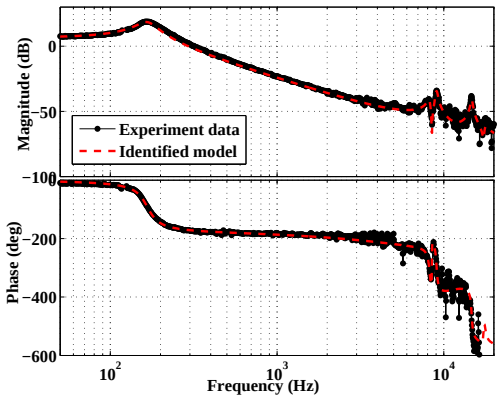

Figure 3: VCM FREQUENCY RESPONSE

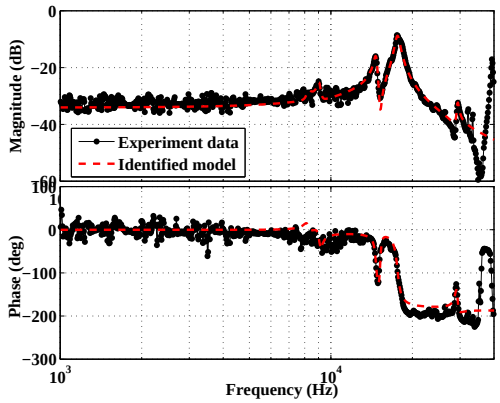

Figure 4: PZT MICRO-ACTUATOR FREQUENCY RESPONSE

As illustrated in [8], we separately fitted a continuous-time model to each of these frequency responses of the VCM and MA, which are shown in Fig 3 and Fig. 4 respectively. Then, we combined the fitted models into a single model and used common mode identification [3] to eliminate redundant copies of the suspension vibration modes. As a result, the continuous-time model for the nominal plant G_p is given by

$$G_p(s) = \begin{bmatrix} -0.8 & 6.6 \end{bmatrix} \times 10^{-4} + \sum_{i=1}^{6} \begin{bmatrix} 1 & 0 \end{bmatrix} \left(sI - \begin{bmatrix} 2\zeta_i\omega_i & 1 \\ \omega_i^2 & 0 \end{bmatrix} \right)^{-1} B_i \tag{1}$$

where the model parameters are as listed in Table 1.

2.2 Dual-stage Servo Control Systems

We rewrite the dual-stage servo system as the linear fractional transformation (LFT) shown in Fig. 5. In Fig. 5, z_2 is "performance monitoring" output with the control input weighting values of W_{u_v} and W_{u_p}

Table 1: Model PARAMETERS FOR G_p

mode, i	$\omega_i(\times 10^5)$	ζ_i	B_i
1	0.0105	0.1270	$\begin{bmatrix} -59.2235 & 0 \\ 2.3315e5 & 0 \end{bmatrix}$
2	0.5172	0.0225	$\begin{bmatrix} 21.03 & -19.2637 \\ -2.9736e5 & 7.7326e5 \end{bmatrix}$
3	0.5691	0.0151	$\begin{bmatrix} 13.5775 & -32.4137 \\ -1.7524e6 & -2.0289e6 \end{bmatrix}$
4	0.9235	0.0145	$\begin{bmatrix} -4.2638 & 108.1704 \\ 2.1956e6 & -3.5665 \end{bmatrix}$
5	1.1067	0.0216	$\begin{bmatrix} 0.748 & 38.0032 \\ 3.4651e5 & -1.9294e8 \end{bmatrix}$
6	1.8435	0.0094	$\begin{bmatrix} 1.5431 & 37.9309 \\ 2.7582e5 & -6.4101e6 \end{bmatrix}$

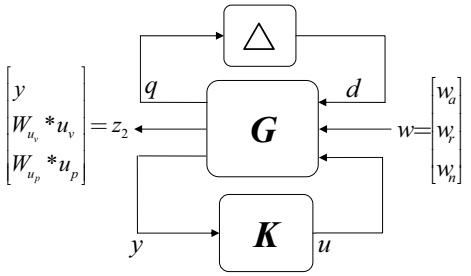

Figure 5: DUAL-STAGE HDD SERVOS IN LFT REPRESENTATION.

for VCM and MA respectively. Suppose, the open-loop system G and the controller K have the following state-space realization:

$$G \sim \left[\begin{array}{c|ccc} A & B_1 & B_2 & B_3 \\ \hline C_1 & D_{11} & D_{12} & D_{13} \\ C_2 & D_{21} & D_{22} & D_{23} \\ C_3 & D_{31} & D_{32} & 0 \end{array}\right], \; K \sim \left[\begin{array}{c|c} A_c & B_c \\ \hline C_c & D_c \end{array}\right]. \tag{2}$$

3 H_2 GUARANTEED COST ANALYSIS

As mentioned in Section 1, it is desirable to design a controller to achieve robust performance, i.e. the designed controller is able to guarantee an adequate level of performance for a set of hard disk drives. In this section, we utilize the analysis of the robust H_2 performance of an uncertain discrete-time linear time-invariant (LTI) system in [2] to establish an upper bound on the worst-case H_2 performance of an uncertain system. Such an upper bound will be employed to formulate H_2 guaranteed cost control problem in next

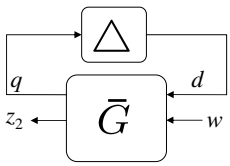

Figure 6: UPPER LFT REPRESENTATION WITH UNCERTAINTY.

section.

3.1 H_2 Guaranteed Cost

We consider the uncertain system $\bar{G}$ and its uncertainty Δ as illustrated in Fig. 6. Throughout this paper, we denote the upper LFT of $\bar{G}$ by Δ as $\mathcal{F}_u(\bar{G}, \Delta)$, as shown in Fig. 6. Suppose, Δ is a norm-bounded unstructured uncertainty with $\|\Delta\|_\infty \leq 1$ and $\bar{G}$ has the state-space realization

$$\bar{G} \sim \left[\begin{array}{c|cc} \bar{A} & \bar{B}_1 & \bar{B}_2 \\ \hline \bar{C}_1 & \bar{D}_{11} & \bar{D}_{12} \\ \bar{C}_2 & \bar{D}_{21} & \bar{D}_{22} \end{array}\right] . \tag{3}$$

From [4], we know that $\|\mathcal{F}_u(\bar{G}, \Delta)\|_2^2 < \gamma,\ \forall \|\Delta\|_\infty \leq 1$ if there exist $\tau > 0, P \succ 0, W, V$ such that $\mathrm{tr}\{W\} < \gamma$ and

$$\mathcal{M}_{\bar{G}}(\tau, P, W, V) := \left[\begin{array}{ccc} P & 0 & V^T \\ 0 & \tau I & 0 \\ V & 0 & W \end{array}\right] - \left[\begin{array}{ccc} \bar{A} & \bar{B}_1 & \bar{B}_2 \\ \bar{C}_1 & \bar{D}_{11} & \bar{D}_{12} \\ \bar{C}_2 & \bar{D}_{21} & \bar{D}_{22} \end{array}\right]^T \left[\begin{array}{ccc} P & 0 & 0 \\ 0 & \tau I & 0 \\ 0 & 0 & I \end{array}\right] \left[\begin{array}{ccc} \bar{A} & \bar{B}_1 & \bar{B}_2 \\ \bar{C}_1 & \bar{D}_{11} & \bar{D}_{12} \\ \bar{C}_2 & \bar{D}_{21} & \bar{D}_{22} \end{array}\right] \succ 0.$$

This sufficient condition for $\|\mathcal{F}_u(\bar{G}, \Delta)\|_2^2 < \gamma,\ \forall \|\Delta\|_\infty \leq 1$ motivates us to consider the following optimization

$$J_\tau(\bar{G}) := \inf_{P,W,V} tr\{W\} \quad \text{s.t. } P \succ 0,\ \mathcal{M}_{\bar{G}}(\tau, P, W, V) \succ 0 \ . \tag{4}$$

When (4) is infeasible for a particular value of $\tau > 0$, we use the convention that $J_\tau(\bar{G}) = \infty$. Then, $J_\tau(\bar{G})$ turns out to be an upper bound of the worst-case H_2 norm with the uncertainty, i.e.,

$$J_\tau(\bar{G}) \geq \sup_{\|\Delta\|_\infty \leq 1} \left\|\mathcal{F}_u(\bar{G}, \Delta)\right\|_2^2 \ .$$

In order to reduce the difference between the upper bound and the worst-case H_2 norm, we consider the following optimization to minimize the upper bound:

$$\inf_{\tau>0} J_\tau(\bar{G}) \; . \tag{5}$$

Notice that the square root of the value of (5) is called H_2 guaranteed cost for the system $\bar{G}$ shown in Fig. 6. In addition, the H_2 guaranteed cost given by (5) is finite if and only if the system is robustly stable and this can be checked using a single Riccati equation [2].

3.2 H_2 Guaranteed Cost Computation

For a given system $\bar{G}$ in (3), we define

$$\begin{aligned}
\bar{Q} &:= \tau \bar{C}_1^T \bar{C}_1 + \bar{C}_2^T \bar{C}_2, & \bar{R} &:= \tau(\bar{D}_{11}^T \bar{D}_{11} - I) + \bar{D}_{21}^T \bar{D}_{21} \\
\bar{S} &:= \tau \bar{C}_1^T \bar{D}_{11} + \bar{C}_2^T \bar{D}_{21}, & \bar{Q}_W &:= \tau \bar{D}_{12}^T \bar{D}_{12} + \bar{D}_{22}^T \bar{D}_{22} \\
\bar{S}_W &:= \tau \bar{D}_{12}^T \bar{D}_{11} + \bar{D}_{22}^T \bar{D}_{21}, & \bar{\phi} &:= (\bar{A}, \bar{B}, \bar{Q}, \bar{R}, \bar{S}) \\
\bar{\psi} &:= (\bar{B}_2, \bar{B}_1, \bar{Q}_W, \bar{R}, \bar{S}_W) & & \\
\mathcal{R}_{\bar{\phi}}(P) &:= \bar{A}^T P \bar{A} + \bar{Q} - (\bar{A}^T P \bar{B} + \bar{S})(\bar{B}^T P \bar{B} + \bar{R})^{-1}(\bar{B}^T P \bar{A} + \bar{S}^T) & & \\
\mathcal{K}_{\bar{\phi}}(P) &:= -(\bar{B}^T P \bar{B} + \bar{R})^{-1}(\bar{B}^T P \bar{A} + \bar{S}^T) & & \\
\mathcal{A}_{\bar{\phi}}(P) &:= \bar{A} + \bar{B}\mathcal{K}_{\bar{\phi}}(P) & &
\end{aligned}$$

In [2], we have developed an algorithm to compute the upper bound $J_\tau(\bar{G})$ as follows.

Algorithm 1 *The following algorithm computes $J_\tau(\bar{G})$ under the assumption that A is Schur.*

1. *Find the stabilizing solution of the DARE $P_0 = \mathcal{R}_{\bar{\phi}}(P_0)$*
2. *Compute the Cholesky factorization $LL^T = -(\bar{B}_1^T P_0 \bar{B}_1 + R)$*
3. *$\check{K} = L \backslash (\bar{B}_1^T P_0 \bar{B}_2 + \bar{S}_W^T)$*
4. *$J_\tau(\bar{G}) = \mathrm{sum}(P_0 \circ (\bar{B}_2 \bar{B}_2^T)) + \tau \|\bar{D}_{12}\|_F^2 + \|\bar{D}_{22}\|_F^2 + \|\check{K}\|_F^2$*

If either of the first two steps fail, then $J_\tau(\bar{G}) = \infty$. □

Notice that "$\circ$" represents the Hadamard product (i.e. element-wise multiplication) for two matrices, the operator "sum" will take the sum of all elements of a matrix, and $\| * \|_F$ denotes the Frobenius norm of a

matrix "*". In addition, we say a matrix is Schur if all of its eigenvalues lie strictly inside the unit disk in the complex plane.

In [2], we also have developed an algorithm to compute $\frac{d}{d\tau}(J_\tau(\bar{G}))$ as follows.

Algorithm 2 *The following algorithm computes* $\frac{d}{d\tau}(J_\tau(\bar{G}))$.

1. *Use Algorithm 1 to compute* $P_0, L, \check{K}, J_\tau(\bar{G})$
2. $\mathcal{K}_{\bar{\phi}}(P_0) = L^T \backslash (L \backslash (\bar{B}_1^T P_0 \bar{A} + \bar{S}^T))$
3. $\mathcal{A}_{\bar{\phi}}(P_0) = \bar{A} + \bar{B}_1 \mathcal{K}_{\bar{\phi}}(P_0)$
4. $Q_{Lyap} = (\bar{C}_1 + \bar{D}_{11}\mathcal{K}_{\bar{\phi}}(P_0))^T(\bar{C}_1 + \bar{D}_{11}\mathcal{K}_{\bar{\phi}}(P_0)) - \mathcal{K}_{\bar{\phi}}(P_0)^T \mathcal{K}_{\bar{\phi}}(P_0)$
5. *Solve the discrete Lyapunov equation*

$$\frac{dP_0}{d\tau} = \mathcal{A}_{\bar{\phi}}(P_0)^T \frac{dP_0}{d\tau} \mathcal{A}_{\bar{\phi}}(P_0) + Q_{Lyap}$$

6. $\mathcal{K}_{\bar{\psi}}(P_0) = L^T \backslash \check{K}$
7. $\mathcal{A}_{\bar{\psi}}(P_0) = \bar{B}_2 + \bar{B}_1 \mathcal{K}_{\bar{\psi}}(P_0)$
8. $\frac{d}{d\tau}(J_\tau(\bar{G})) = \mathrm{sum}\left(\frac{dP_0}{d\tau} \circ \left(\mathcal{A}_{\bar{\psi}}(P_0)\mathcal{A}_{\bar{\psi}}(P_0)^T\right)\right) + \|\bar{D}_{12} + \bar{D}_{11}\mathcal{K}_{\bar{\psi}}(P_0)\|_F^2 - \|\mathcal{K}_{\bar{\psi}}(P_0)\|_F^2$

□

For the control synthesis algorithm presented in next section, the following algorithm has been developed in [2] to compute the H_2 guaranteed cost in (5).

Algorithm 3 *The following algorithm computes the* H_2 *guaranteed cost of* $\bar{G}$.

1. ***Check Finiteness of the*** H_2 ***Guaranteed Cost:*** *Verify that the system is robustly stable using a Riccati equation to check its* H_∞ *norm.*
2. ***Find Initial Interval:*** *Choose* $\alpha > 1$. *Starting from* $k = 0$, *iterate over* k *until a value of* $\tau = \alpha^k$ *is found such that* $J_\tau(\bar{G}) \neq \infty$ *and* $(d/d\tau)(J_\tau(\bar{G})) > 0$. *Denote this value of value of* τ *by* τ_u; *this corresponds to an upper bound on the optimal value of* τ. *If* $\tau_u = 1$, *then 0 is a lower bound on the optimal value of* τ, *otherwise* τ_u/α *is a lower bound.*
3. ***Bisection:*** *Solve the equation* $(d/d\tau)(J_\tau(\bar{G})) = 0$ *over* τ *using bisection. Whenever* $J_\tau(\bar{G}) = \infty$, *this corresponds to a lower bound on the optimal value of* τ.

In this algorithm, each evaluation of $J_\tau(\bar{G})$ *is done using Algorithm 1 and each evaluation of* $(d/d\tau)(J_\tau(\bar{G}))$ *when* $J_\tau(\bar{G}) \neq \infty$ *is done using Algorithm 2.* □

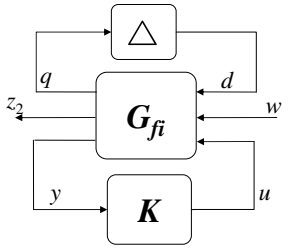

Figure 7: FULL INFORMATION CONTROL STRUCTURE.

4 H_2 GUARANTEED COST CONTROL SYNTHESIS

4.1 Control Problem Formulation

With the H_2 guaranteed cost analysis results in Section 3, we are interested in finding a controller to minimize the upper bound in (4) so as to achieve the optimal H_2 guaranteed cost for the robust performance. Consequently, the H_2 guaranteed cost control design for the servo system shown in Fig. 5 can be transformed to the following optimization

$$\inf_{K} \inf_{\tau>0} J_\tau(\mathcal{F}_l(G,K)) \; . \tag{6}$$

4.2 Full Information Control Algorithm

Before we present the output feedback control synthesis algorithm, we consider the optimal control (in terms of J_τ) of the interconnection shown in Fig. 7. In this diagram, we let G_{fi} have the state-space realization

$$G_{fi} \sim \left[\begin{array}{c|cccc} A & B_1 & B_2 & B_3 \\ \hline C_1 & D_{11} & D_{12} & D_{13} \\ C_2 & D_{21} & D_{22} & D_{23} \\ \begin{bmatrix} I \\ 0 \\ 0 \end{bmatrix} & \begin{bmatrix} 0 \\ I \\ 0 \end{bmatrix} & \begin{bmatrix} 0 \\ 0 \\ I \end{bmatrix} & \begin{bmatrix} 0 \\ 0 \\ 0 \end{bmatrix} \end{array}\right] \; . \tag{7}$$

From the state-space realization in (7), we learn that the feedback controller has the full access to the plant state and disturbances. Thus, the control design of G_{fi} is called full information control problem.

As discussed in [2], we consider the optimal full information control problem corresponding to solving

the optimization problem

$$J_{fi,\epsilon} := \inf_K J_{(\epsilon^{-1})}(\mathcal{F}_l(G_{fi}, K)) \ . \tag{8}$$

A few quantities which will be important in this section are the combinations of state-space matrices

$$B_{[1,3]} := \begin{bmatrix} B_1 & B_3 \end{bmatrix}, \qquad C := \begin{bmatrix} C_1 \\ C_2 \end{bmatrix}, \qquad D_1 := \begin{bmatrix} D_{11} \\ D_{21} \end{bmatrix}$$
$$D_2 := \begin{bmatrix} D_{12} \\ D_{22} \end{bmatrix}, \qquad D_3 := \begin{bmatrix} D_{13} \\ D_{23} \end{bmatrix}, \qquad D_{[1,3]} := \begin{bmatrix} D_{11} & D_{13} \\ D_{21} & D_{23} \end{bmatrix}$$

and the parameters

$$Q := C_1^T C_1 + \epsilon C_2^T C_2, \qquad S := C_1^T \begin{bmatrix} D_{11} & D_{13} \end{bmatrix} + \epsilon C_2^T \begin{bmatrix} D_{21} & D_{23} \end{bmatrix}$$
$$\bar{Q} := D_{12}^T D_{12} + \epsilon D_{22}^T D_{22}, \quad \bar{S} := D_{12}^T \begin{bmatrix} D_{11} & D_{13} \end{bmatrix} + \epsilon D_{22}^T \begin{bmatrix} D_{21} & D_{23} \end{bmatrix}$$
$$R := \begin{bmatrix} D_{11}^T D_{11} - I & D_{11}^T D_{13} \\ \bullet & D_{13}^T D_{13} \end{bmatrix} + \epsilon \begin{bmatrix} D_{21}^T D_{21} & D_{21}^T D_{23} \\ \bullet & D_{23}^T D_{23} \end{bmatrix}$$
$$\phi := (A,\ B_{[1,3]},\ Q,\ R,\ S), \quad \psi := (B_2,\ B_{[1,3]},\ \bar{Q},\ R,\ \bar{S})$$

Throughout this paper, the symbol "$\bullet$" denotes the transpose of the corresponding element at its transposed position.

In this section, we will make the following assumptions:

(A1) $D_3^T D_3$ is invertible

(A2) (A, B_3) is stabilizable

(A3) $\dim\left(\mathrm{Ker}\begin{bmatrix} A - \lambda I & B_3 \\ C & D_3 \end{bmatrix}\right) = 0,\ \forall \lambda \in \mathbb{C}$ satisfying $|\lambda| \geq 1$.

Notice that the operator $\mathrm{Ker}(*)$ represents the kernel (i.e. null space) of the matrix "*". These regularity conditions are analogous to those required for the design of a linear quadratic regulator or full information H_∞ controller using discrete Riccati equations [10].

With these formulas in place, we first present two algorithms which respectively compute $J_{fi,\epsilon}$ and its derivative with respect to ϵ.

Algorithm 4 *The following algorithm computes $J_{fi,\epsilon}$, the corresponding optimal controller, and the corresponding optimal closed-loop system under assumptions (A1)–(A3).*

1. *Find the stabilizing solution of the DARE $\mathcal{R}_\phi(P) = P$*
2. *Compute the Cholesky factorization $T_{22}^T T_{22} = B_3^T P_0 B_3 + D_{13}^T D_{13} + \epsilon D_{23}^T D_{23}$*
3. *$T_{21} = T_{22}^T \backslash (B_3^T P_0 B_1 + D_{13}^T D_{11} + \epsilon D_{23}^T D_{21})$*
4. *Compute the Cholesky factorization $T_{11}^T T_{11} = T_{21}^T T_{21} + I - B_1^T P_0 B_1 - D_{11}^T D_{11} - \epsilon D_{21}^T D_{21}$*
5. *Form the optimal controller gains:*

$$
\begin{aligned}
K_x^o &= -T_{22} \backslash (T_{22}^T \backslash (B_3^T P_0 A + D_{13}^T C_1 + \epsilon D_{23}^T C_2)) \\
K_d^o &= -T_{22} \backslash T_{21} \\
K_w^o &= -T_{22} \backslash (T_{22}^T \backslash (B_3^T P_0 B_2 + D_{13}^T D_{12} + \epsilon D_{23}^T D_{22}))
\end{aligned}
$$

6. *Form the closed-loop state-space matrices*

$$
\begin{aligned}
&A^{cl} = A + B_3 K_x^o, \quad B_1^{cl} = B_1 + B_3 K_d^o, \quad B_2^{cl} = B_2 + B_3 K_w^o \\
&C_1^{cl} = C_1 + D_{13} K_x^o,\ D_{11}^{cl} = D_{11} + D_{13} K_d^o,\ D_{12}^{cl} = D_{12} + D_{13} K_w^o \\
&C_2^{cl} = C_2 + D_{23} K_x^o,\ D_{21}^{cl} = D_{21} + D_{23} K_d^o,\ D_{22}^{cl} = D_{22} + D_{23} K_w^o
\end{aligned}
$$

7. *Verify that A^{cl} is Schur*
8. $\check{K} = T_{11}^T \backslash \Big((B_1^{cl})^T P_0 B_2^{cl} + (D_{11}^{cl})^T D_{12}^{cl} + \epsilon (D_{21}^{cl})^T D_{22}^{cl} \Big)$
9. $J_{fi,\epsilon} = \epsilon^{-1} \Big(\mathrm{sum}(P_0 \circ [B_2^{cl} (B_2^{cl})^T]) + \|D_{12}^{cl}\|_F^2 + \epsilon \|D_{22}^{cl}\|_F^2 + \|\check{K}\|_F^2 \Big)$

If steps 1, 2, or 4 fail or if A^{cl} is found to be not Schur in step 7, then $J_{fi,\epsilon} = \infty$ and there is no optimizing controller. □

Algorithm 5 *The following algorithm computes $dJ_{fi,\epsilon}/d\epsilon$.*

1. *Use Algorithm 4 to compute the following quantities: P_0, T_{11}, T_{21}, T_{22}, K_x^o, K_d^o, K_w^o, A^{cl}, B_1^{cl}, B_2^{cl}, C_1^{cl}, C_2^{cl}, D_{11}^{cl}, D_{12}^{cl}, D_{21}^{cl}, D_{22}^{cl}, $\check{K}$, and $J_{fi,\epsilon}$*

2. *Compute the quantities*

$$K_{dx} = T_{11} \backslash \left(T_{11}^T \backslash [(B_1^{cl})^T P_0 A + (D_{11}^{cl})^T C_1 + \epsilon (D_{21}^{cl})^T C_2] \right)$$
$$K_{dw} = T_{11} \backslash \left(T_{11}^T \backslash [(B_1^{cl})^T P_0 B_2 + (D_{11}^{cl})^T D_{12} + \epsilon (D_{21}^{cl})^T D_{22}] \right)$$

3. *Compute the quantities*

$$\bar{K}_x = K_x^o + K_d^o K_{dx}$$
$$\bar{K}_w = K_w^o + K_d^o K_{dw}$$

4. *Compute the quantities*

$$\mathcal{A}_\phi(P_0) = A + B_1 K_{dx} + B_3 \bar{K}_x, \; \mathcal{A}_\psi(P_0) = B_2 + B_1 K_{dw} + B_3 \bar{K}_w$$
$$\check{C} = C_2 + D_{21} K_{dx} + D_{23} \bar{K}_x, \; \check{D} = D_{22} + D_{21} K_{dw} + D_{23} \bar{K}_w$$

5. *Using the MATLAB function* `dlyapchol`*, solve for the Cholesky factor* U *in the discrete Lyapunov equation* $U^T U = \mathcal{A}_\phi(P_0)^T (U^T U) \mathcal{A}_\phi(P_0) + \check{C}^T \check{C}$

6. $dJ_{fi,\epsilon}/d\epsilon = \epsilon^{-1}(\|U\mathcal{A}_\psi(P_0)\|_F^2 + \|\check{D}\|_F^2 - J_{fi,\epsilon})$ □

With these results in place, we can easily solve (8) using the following algorithm:

Algorithm 6 *The following algorithm computes the optimal* H_2 *guaranteed cost of the closed-loop system along with an optimal controller.*

1. ***Check Regularity Conditions:*** *Verify that assumptions (A1)–(A3) hold.*

2. ***Find Initial Interval:*** *Choose* $\alpha > 1$*. Check if* $J_{fi,\epsilon} \neq \infty$ *and* $dJ_{fi,\epsilon}/d\epsilon < 0$ *when* $\epsilon = 1$*. If so, start from* $k = 1$ *and increment* k *until either or these conditions fail to be met when* $\epsilon = \alpha^k$*. Denoting the corresponding value of* ϵ *as* ϵ_u*, there exists an optimal value of* ϵ *in the interval* $(\alpha^{-1}\epsilon_u, \epsilon_u)$*.*

   If instead either $J_{fi,\epsilon} = \infty$ *or* $dJ_{fi,\epsilon}/d\epsilon > 0$ *when* $\epsilon = 1$*, start from* $k = 1$ *and increment* k *until* $J_{fi,\epsilon} \neq \infty$ *and* $dJ_{fi,\epsilon}/d\epsilon < 0$ *when* $\epsilon = \alpha^{-k}$*. Denoting the corresponding value of* ϵ *as* ϵ_l*, there exists an optimal value of* ϵ *in the interval* $(\epsilon_l, \alpha\epsilon_l)$*.*

3. ***Bisection:*** *Solve* $dJ_{fi,\epsilon}/d\epsilon = 0$ *over* ϵ *using bisection. Whenever* $J_{fi,\epsilon} = \infty$ *for a particular value of* ϵ*, this value of* ϵ *is an upper bound on the optimal value of* ϵ*.*

In this algorithm, each evaluation of $J_{fi,\epsilon}$ is done using Algorithm 4 and each evaluation of $dJ_{fi,\epsilon}/d\epsilon$ when $J_{fi,\epsilon} \neq \infty$ is done using Algorithm 5. □

4.3 Full Control Algorithm

In [2], the output feedback control problem in (6) is reduced to the following optimal full control problem

$$\inf_{\tilde{K}} J_1(\mathcal{F}_l(G_4, \tilde{K})) \tag{9}$$

where G_4 has the following the state-space realization

$$G_4 \sim \left[\begin{array}{c|ccc} A + B_1 K_{dx} & B_1 T_{11}^{-1} & B_2 + B_1 K_{dw} & I & 0 \\ \hline -T_{22}\bar{K}_x & -T_{22} K_d^o T_{11}^{-1} & -T_{22}\bar{K}_w & 0 & T_{22} \\ 0 & 0 & 0 & 0 & 0 \\ C_3 + D_{31} K_{dx} & D_{31} T_{11}^{-1} & D_{32} + D_{31} K_{dw} & 0 & 0 \end{array}\right] \tag{10}$$

where the parameters K_{dx}, K_{dw}, $\bar{K}_x$, and $\bar{K}_w$ are defined in Algorithm 5.

It is not currently known whether or not the optimal full control problem can be solved using Riccati equations. Therefore, to solve this problem, we will resort to the SDP approach. In particular, we have proved that the optimization problem (9) is equivalent to the optimization problem

$$\inf_{P,W,V,\hat{L}_x,L_v} \operatorname{tr}\{W\} \quad \text{s.t.} \tag{11a}$$

$$\left[\begin{array}{ccccc} P & \bullet & \bullet & \bullet & \bullet \\ 0 & T_{11}^T T_{11} & \bullet & \bullet & \bullet \\ V & 0 & W & \bullet & \bullet \\ P\check{A} + \hat{L}_x \check{C} & PB_1 + \hat{L}_x D_{31} & P\check{B} + \hat{L}_x \check{D} & P & \bullet \\ T_{22}(L_v \check{C} - \bar{K}_x) & T_{22}(L_v D_{31} - K_d^o) & T_{22}(L_v \check{D} - \bar{K}_w) & 0 & I \end{array}\right] \succ 0 \tag{11b}$$

where

$$\left[\begin{array}{cc} \check{A} & \check{B} \\ \check{C} & \check{D} \end{array}\right] := \left[\begin{array}{cc} A + B_1 K_{dx} & B_2 + B_1 K_{dw} \\ C_3 + D_{31} K_{dx} & D_{32} + D_{31} K_{dw} \end{array}\right]. \tag{12}$$

Consequentially, for any $P, W, V, \hat{L}_x, L_v$ that satisfy (11b), an output feedback controller which achieves

$J_\tau(\mathcal{F}_l(G,K)) \leq J_{fi,\epsilon} + \epsilon^{-1}\mathrm{tr}\{W\}$ can be reconstructed from

$$\begin{aligned} A_c &= A + B_1 K_{dx} + B_3 \bar{K}_x + (P^{-1}\hat{L}_x - B_3 L_v)(C_3 + D_{31} K_{dx}) \\ K &\sim \left[\begin{array}{c|c} A_c & P^{-1}\hat{L}_x - B_3 L_v \\ \hline L_v(C_3 + D_{31}K_{dx}) - \bar{K}_x & L_v \end{array}\right]. \end{aligned} \tag{13}$$

4.4 Output Feedback Control Algorithm

This section gives a heuristic for solving (6) using the results presented so far in this paper.

Algorithm 7 *The following algorithm is a heuristic for solving the optimal output feedback control problem* (6)*.*

1. ***Find Initial Value of*** τ

   (a) ***Full Information Controller Design:*** *Using Algorithm 6, design an optimal full information controller.*

   (b) ***Find Feasible Value of*** τ***:*** *Choose* $\alpha > 0$*. For the final values determined during the last full information controller design, solve* (11) *using an SDP solver. If the optimization was feasible, reconstruct the corresponding output feedback controller* K *using* (13)*. If the optimization was not feasible, set* $\tau \leftarrow \alpha\tau$*, design a full information controller for* $\epsilon = \tau^{-1}$ *using Algorithm 4, and redo this step.*

   (c) ***Closed-Loop System Analysis (Fixed*** K***):*** *Form the closed-loop system* $\mathcal{F}_l(G,K)$ *and analyze its* H_2 *guaranteed cost performance using Algorithm 3.*

2. ***Controller Design***

   (a) ***Output Feedback Controller Design (Fixed*** τ***):*** *For the value of* $\tau > 0$ *found in the previous closed-loop system analysis step, solve* (11) *using an SDP solver and reconstruct the corresponding controller* K *using* (13)*.*

   (b) ***Closed-Loop System Analysis (Fixed*** K***):*** *Form the closed-loop system* $\mathcal{F}_l(G,K)$ *and analyze its* H_2 *guaranteed cost performance using Algorithm 3. Return to step 2a.* □

In our implementation, we use $\alpha = 100$. We use two stopping criteria in this algorithm. If the number of output feedback controller optimizations (i.e. the number of times steps 1b and 2a have been executed) exceeds 30 or if $J_{of}^{[i-1]}/J_{of}^{[i]} - 1 < 10^{-4}$ where $J_{of}^{[i]}$ is the cost reported the i^{th} time step 2b executes, we terminate the algorithm. We also terminate the algorithm if the SDP solver claims infeasibility in step 2a.

5 CONTROL IMPLEMENTATION

5.1 H_2 Guaranteed Cost Control Design

For the dual-stage track-following servo design shown in Fig. 2, we need to design a proper uncertainty weighting function W_Δ so that the modeling of the uncertain plant, $(1+W_\Delta\Delta)G_p$, covers all plant variations but is not too conservative. Based on the servo system identification in [8], the uncertainty weighting function was selected as shown in Fig. 8. The selected uncertainty weighting function demonstrates that the real plant could have an unstructured uncertainty of a $\pm 2\%$ gain variation at low frequency and a $\pm 54\%$ gain variation at high frequency respectively from the nominal plant.

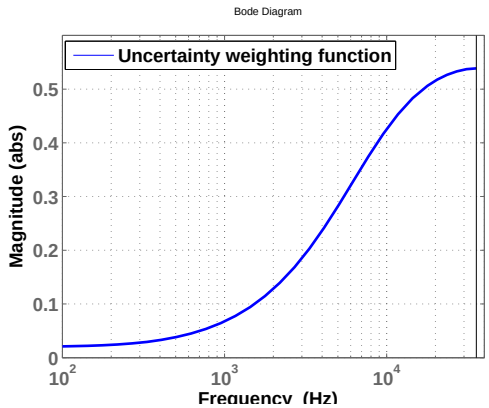

Figure 8: PLANT UNCERTAINTY WEIGHTING FUNCTION W_Δ

With the control input weighting values of $W_{u_v} = W_{u_p} = 0.04$, the H_2 guaranteed cost control is synthesized by using Algorithm 7. As demonstrated in [4, 6], the proposed control algorithm, by exploiting the Riccati equation structure to decrease the number and complexity of SDPs, is able to increase the computation speed and accuracy compared to the approaches [5] solving LMIs.

5.2 Experimental Study

Figure 9 shows a picture of the experimental setup. A PZT-actuated suspension shown in Fig. 1 was assembled to an arm of the E-block of a commercial 3.5" 7200 RPM disk drive. An LDV was utilized to measure the absolute radial displacement of the slider. The resolution of the LDV is 2 nm for the measurement gain of 0.5 μ/V. The control circuits include a Texas Instrument TMS320C6713 DSP board and an in-house made analog board with a 12-bit ADC, a 12-bit DAC, a voltage amplifier to drive the MA, and a current amplifier to drive the VCM. The DSP sampling frequency is 71.4 KHz in this paper. And the input delay including ADC and DAC conversion delay and DSP computation delay is 6 μs. A hole was cut

through the case of the drive to make laser go into the drive.

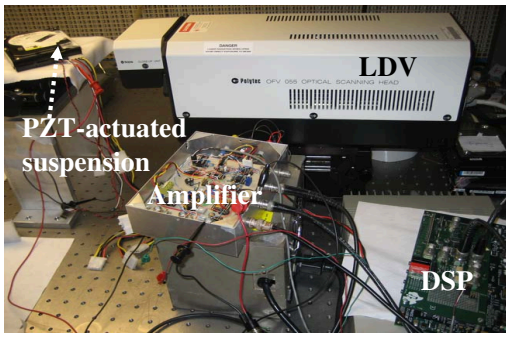

Figure 9: DSA EXPERIMENT SETUP

Then, the synthesized controller was implemented on our experiment setup illustrated in Fig. 9. In order to validate our control design, the closed-loop sensitivity function by using the sinusoidal sweeping signal was measured. The observed sensitivity function is indicated by the black line in Fig. 10, while the predicted one is indicated by the red line. Note that the predicted sensitivity function ($T_s = \frac{1}{1+G_pK}$) was calculated using the controller transfer function and measured open-loop plant transfer functions. From the experiment results, we see the predicted and observed closed-loop sensitivity functions agree very well especially at frequencies below 1 KHz. The predicted sensitivity function at frequencies above 1 KHz is very noisy, because the measured MA frequency response is quite noise, as shown in Fig. 4. From the results in Fig. 10, we also see that the observed sensitivity transfer function matches the base line (in the sense of average) of the predicted one from 1 KHz to 3 KHz. In addition, the experiment results demonstrate that the designed controller using our presented H_2 guaranteed cost control synthesis algorithm produced a relatively-high gain-crossover frequency of 3 KHz for the error rejection function.

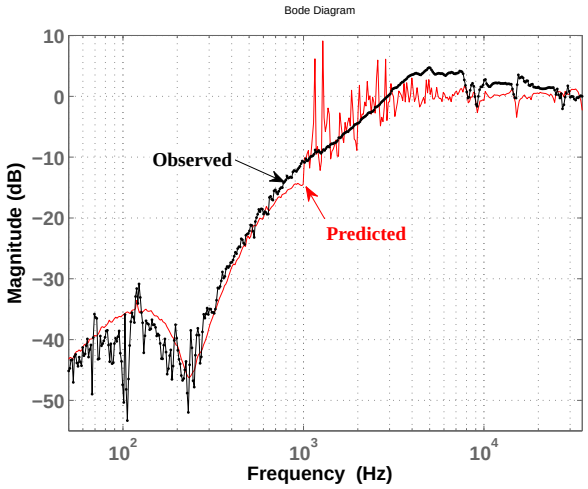

Figure 10: EXPERIMENT RESULTS FOR ERROR REJECTION FUNCTIONS

6 CONCLUSION

In this paper, we first presented an upper bound, H_2 guaranteed cost, for the worst-case H_2 performance of a discrete-time system with a norm-bounded unstructured uncertainty. Based on the H_2 guaranteed cost analysis and the corresponding optimal full information control, we reviewed the output feedback H_2 guaranteed cost control algorithm by exploiting Riccati equation structure to reduce the number and complexity of the SDPs that need to be solved. Consequently, the presented control algorithm is able to increase the computation speed and accuracy compared to the approaches entirely based on semi-definite programs. Then, we applied the proposed control algorithm to dual-stage HDD track-following servo systems. The experiment results by implementing the synthesized controller on an actual disk drive with a PZT-actuated suspension demonstrate the effectiveness of the presented H_2 guaranteed cost control algorithm and validate our control design. Specifically, the designed dual-stage servo by our proposed control synthesis algorithm attained a relatively-high gain-crossover frequency of 3 KHz for the error rejection function.

Acknowledgment

The authors thank Western Digital Inc. and Hutchinson Technology Inc. with parts and valuable information to perform this study. This work was performed with support from the Information Storage Industry Consortium (INSIC) and UC Berkeley Computer Mechanics Laboratory (CML).

References

[1] D. Abramovitch and G. Franklin. A brief history of disk drive control. *IEEE Control Systems Magazine*, 22(3):28–42, 2002.

[2] R. Conway. *Discrete-Time H_2 Guaranteed Cost Control*. PhD Thesis, Univeristy of California Berkeley, Berkeley, CA, 2011.

[3] R. Conway, S. Felix, and R. Horowitz. Model reduction and parametric uncertainty identification for robust h2 control synthesis for dual-stage hard disk drives. *IEEE Transactions on Magnetics*, 43(9):3763–3768, 2007.

[4] R. Conway and R. Horowitz. Analysis of h_2 guaranteed cost performance. In *Proc. of the 2009 Dynamic Systems and Control Conference*, 2009.

[5] R. Conway and R. Horowitz. Guaranteed cost control for linear periodically time-varying systems with structured uncertainty and a generalized H_2 objective. *Mechatronics*, 20(1):12–19, 2010.

[6] R. Conway and R. Horowitz. Optimal full information H_2 guaranteed cost control of discrete-time systems. In *Proc. of the 2010 Dynamic Systems and Control Conference*, 2010.

[7] Y. Li and R. Horowitz. Mechatronics of electrostatic microactuators for computer disk drive dual-stage servo systems. *IEEE/ASME Trans. Mechatronics*, 6(2):111–121, 2001.

[8] J. Nie and R. Horowitz. Design and implementation of dual-stage track-following control for hard disk drives. In *Proc. of the 2009 Dynamic Systems and Control Conference*, 2009.

[9] D. Peaucelle, Y. Ebihara, and D. Arzelier. Robust H_2 perfomance of discrete-time periodic systems: Lmis with reduced dimensions. In *Proc. of the 17th World Congress*, volume **17**. International Fedration of Automatic Control, IFAC, 2008.

[10] M. A. Peters and P. A. Iglesias. *Minimum Entropy Control for Time-Varying Systems. Systems & Control: Foundations & Applications*. Birkhäuser, Boston, MA, 1997.